4th IMEKO TC 18 Symposium
Measurement, Analysis and Modelling of Human Functions
June 14–16, 2010, Prague, Czech Republic

MOTION MEASUREMENT OF TWO-WHEELED SKATEBOARD AND SINUSOIDAL APPROXIMATION OF INPUT FORCE TRAJECTORY

Satoshi Ito, Shouta Takeuchi, Minoru Sasaki

Gifu University (Faculty of Engineering), Gifu, Japan
satoshi@gifu-u.ac.jp, n3128020@edu.gifu-u.ac.jp, sasaki@gifu-u.ac.jp

Abstract – This paper treats a motion generation of the two-wheeled skateboard in order to investigate a propulsion mechanism without leg motions kicking the ground. Human skateboard motions are measured to clarify what kind of rider's motion on the board can produce a propulsion force. To describe this skateboard motion, a reduced order model is derived; whose inputs are wheel orientations, lateral force and yaw moment. Because of the periodicity of the measured motion, large parts of input trajectories are approximated by use of the sinusoidal regression after the frequency analysis. The yaw moment that cannot be measured in our motion measurement system is identified based on computer simulations; whose result is made to be matched to the human skateboard measurement. The coincidence of the time-based trajectories of skateboard motion to the goal direction indicates that some sinusoidal motion can successfully propel this kind of skateboard.

Keywords: Modelling, Two-wheeled skateboard, Motion measurement, Input estimation, Simulation

1. INTORUDUCTION

The mobility brings spatial changes that enlarge the activity space. A wheel system, such as a skateboard [1]-[4], a snakeboard [5]-[14], and so on [15]-[19], is one of possible methods to enhance the mobility.

In this paper, we deal with a kind of wheeled system like a skateboard that has only two wheels, as shown in Fig. 1. Two wheels are attached on the centre line of the board: one is to the front plate while the other is to the rear one. The orientation axes of each wheel are inclined backward, which will limit the moving direction of the board, leftward in this figure. A rider of the board puts the feet on each plate one by one. Thus, the board moves sideways to the rider. To propel the board, the rider repeatedly moves the foot back-and-forth on the board, which provides the yaw moment to the board. On the other hand, two plates are twisted each other around the roll axis by changing the action point of the body weight at each foot. This twist affects the orientation of the two wheels.

Due to the instability in the side direction, such back-and-forth motions of the feet must be achieved with balancing. Because we are investigating a static balance control [20], our original motivation of this work was to propose a method to achieve a spatial change under a static balance: the static balance means that the spatial position of the feet is maintained in contact on the ground, in other words, the leg action kicking to the ground is not used. However, we here especially focus on the propulsion mechanism of this skateboard system without considering a balance, since this mechanism is more important from the viewpoint of the manoeuvrability. To simulate the propulsion dynamics, we investigate how the forces are applied to the board from a rider on it by measuring its motion.

2. METHODS

2.1 Steps for Analysis

The following steps taken in this paper are based on both motion measurements and dynamical simulations:

(1) The two-wheeled skateboard is described using a reduced-order model in order to focus only on the propulsion mechanism of the board, whose inputs are yaw moment, normal force, and wheel direction.
(2) To identify inputs that enable successful board propulsion, human skateboard motions are measured.
(3) Trajectories of the inputs except the yaw moment (the yaw moment cannot be measured in our measurement setup) are constructed from the measurement data.

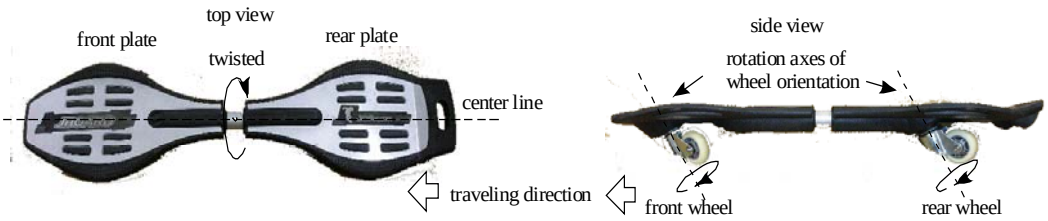

Fig. 1. Two-wheeled Skateboard.

(4) These input trajectories are applied to computer simulations of a reduced-order model.
(5) Then, parameters of the yaw moment are selected, so that the simulation results match the measured data well.
Using these steps, we clarify the inputs from the rider in the form of time-varying trajectories.

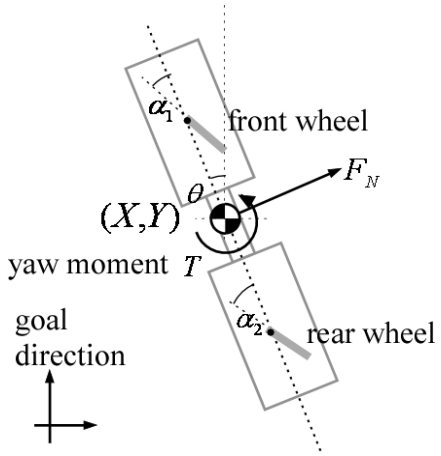

Fig.2. A reduced order model.

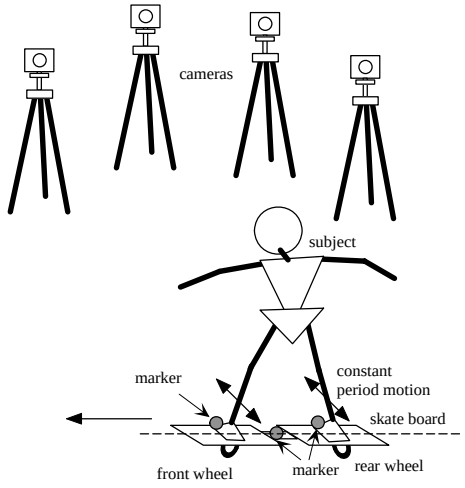

Fig. 3. Measurement setup.

2.2 A reduced-order model

The followings are assumed: the lateral balance of the board is always maintained by the rider's waist-joint motion, independent of the propulsion. In addition, the wheel orientations are regarded as input, because they are directly controlled through the board's twist caused by the weighted shift of the rider's feet.

These assumptions allow us to describe the board dynamics as a reduced-order model without twist, ignoring the lateral balance, as shown in Fig. 2. In this model, inputs are the wheel orientations α_1 and α_2, a yaw moment T and normal force F_N to the board. Note here that the back-and-forth motion of the rider's feet never produces force tangential to the board.

2.3 Motion measurements

To identify the inputs to the board, human skateboard motions were measured using a motion-capture system. This system has four high-speed cameras, which capture 640 × 480 pixel images at 120 frames per second. A flat area of approximately 0.5 m × 3 m was prepared as measurement space, so that all markers would always be captured by at least two cameras. Fig. 3 shows the sketch of our experimental setup.

To detect the board motion, three markers were attached. The first marker was attached to the center of the board, because the center of mass (CoM) of the board is located approximately here (based on the symmetrical board structure). To detect the wheel orientation, the marker should have been attached just above the joint of the two-wheel caster. However, the feet of the subject were placed at this position, so the marker was attached to two toes of the subject.

A 41-year-old male subject, weighing 65 kg, was asked to propel the board from the rest state and then to maintain straight motion until the end of the measurement area for a constant period. Then, the feet of the subject were placed at the center of the two plates, so that the markers were as close to the joint center of the wheel orientation as possible.

Five trials were conducted under the above conditions. These measurements were executed with permission (No. 21-127) from the ethics committee of our organization.

3. ANALYSES AND RESULTS

3.1 Measurement results

From the markers' position in the human skateboard measurements, time-trajectories of α_1, α_2 and F_N are obtained, which are depicted by solid lines in each graph of Fig. 4, Fig. 5 and Fig. 6, respectively. This is the last of the five trials, and the best data in the sense that the period variation of the data in α_1 and α_2 is small, as seen in the next section.

3.2 Input trajectory regression

To utilize computer simulations, each input obtained from motion measurements is reconstructed using regression curves. Sinusoidal functions are used to make regression curves of the measurement data, because the sinusoidal functions are compatible with the frequency analysis we adopt later.

The frequencies are normally the same for all the inputs. Thus, we calculate the following functions for each input:

$$\alpha_1 = \hat{\alpha}_{1A} \sin(2\pi \hat{f} t + \hat{\phi}_1) \tag{1}$$

$$\alpha_2 = -\hat{\alpha}_{2A} \sin(2\pi \hat{f} t + \hat{\phi}_2) \tag{2}$$

$$F_N = \hat{F}_A \sin(2\pi \hat{f} t + \hat{\phi}_F) \tag{3}$$

$$T = \hat{T}_A \sin(2\pi \hat{f} t + \hat{\phi}_F) \tag{4}$$

Here, it is assumed that F_N and T have the same phase shift $\hat{\phi}_F$ because they are originally generated from the same motions, that is, the back-and-forth motions of both feet that are usually a half-period out of phase. The unknown parameters in the above equations are frequency $\hat{f}$, the amplitudes $\hat{\alpha}_{1A}$, $\hat{\alpha}_{2A}$, $\hat{F}_A$, $\hat{T}_A$, and the phase shifts $\hat{\phi}_1$, $\hat{\phi}_2$, $\hat{\phi}_F$.

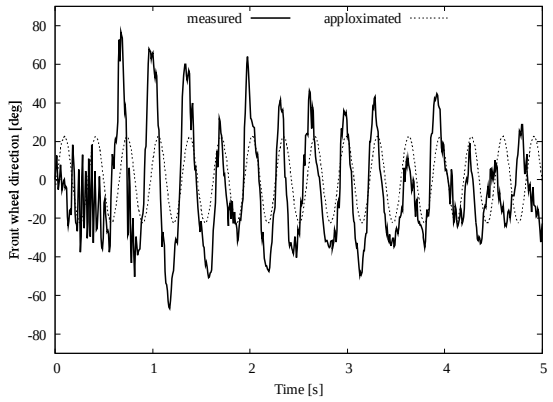

Fig. 4 Measurement result of front wheel orientation α_1

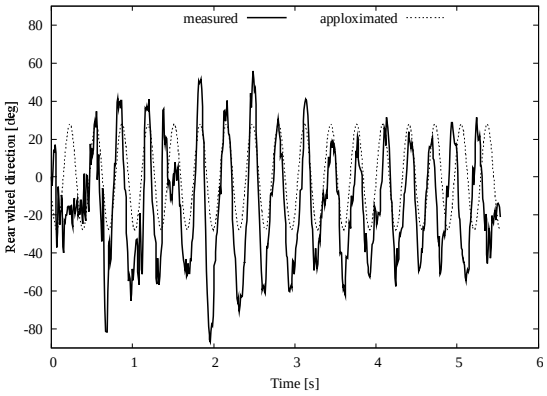

Fig. 5 Measurement result tear wheel orientation α_2

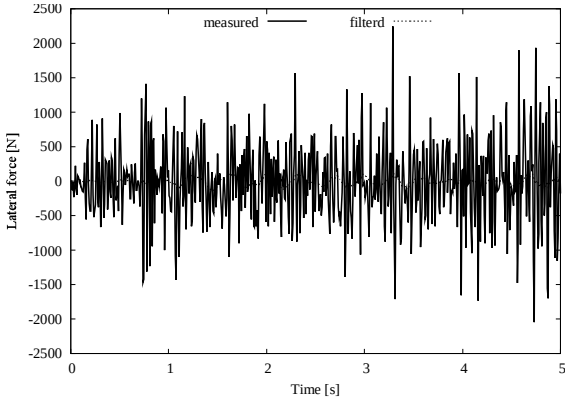

Fig.6 Measurement result of lateral force F_N

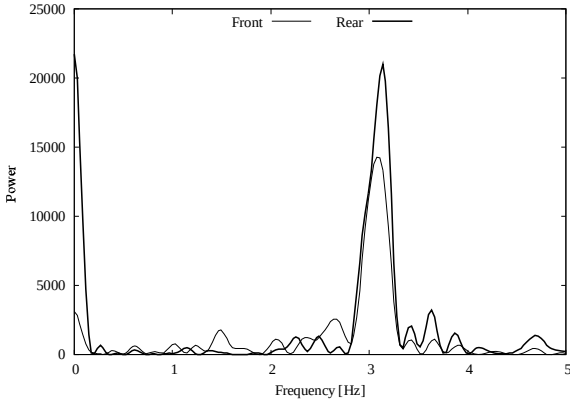

Fig.7 Power Spectrum of wheel orientations

Table 1. Estimated parameters

	$\hat{f}$ [Hz]	$\hat{\phi}_1$ [deg]	$\hat{\phi}_2$ [deg]	$\hat{\phi}_F$ [deg]	$\hat{\alpha}_{1A}$ [deg]	$\hat{\alpha}_{2A}$ [deg]	$\hat{F}_A$ [N]	$\hat{T}_A$ [Nm]
1st	2.9	138.4	147.7	190.4	15.0	32.1	105.5	-10.1
2nd	2.9	114.3	140.8	132.3	23.3	32.9	-34.1	4.7
3rd	2.9	0.0	43.3	8.7	21.5	19.6	-33.4	3.0
4th	2.5	51.8	29.5	37.5	11.6	12.4	13.8	6.7
5th	3.1	-15.2	19.0	-5.1	22.4	27.8	-33.8	3.8

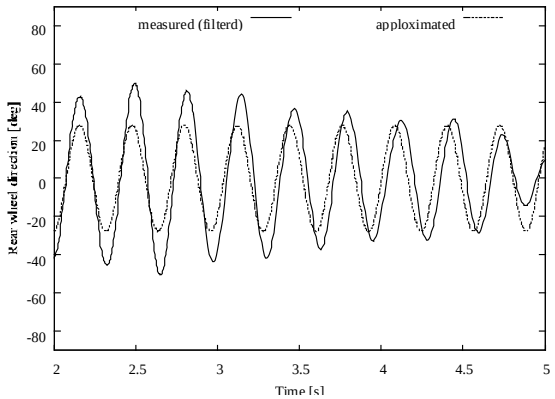

Fig.8 Reconstruction of front wheel orientation.

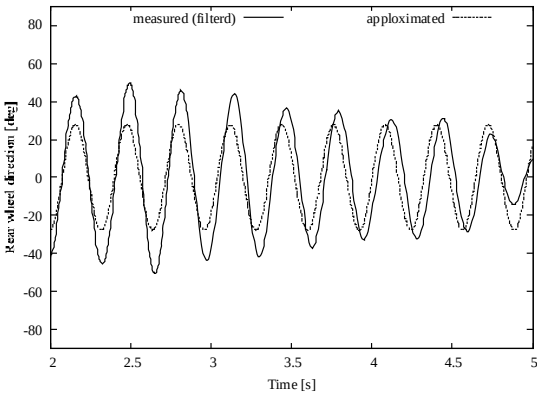

Fig.9 Reconstruction of rear wheel orientation.

3.3 Unknown parameter estimation

In order to identify the frequency of the motion, spectrum analysis was performed for the data of the two wheel orientations. The results are shown in Figure 7.

Next, the phase shifts were identified based on cross-correlation. Each input data was filtered through a two-order band-pass filter, whose peak frequency was set to the identified one, and then cross-correlated to the sine wave with a phase shift of zero at 0 s. The maximal point of the cross-correlation value was selected as the phase shift of the data.

Finally, the amplitude was identified using least mean square method that minimizes the squared sum of the error between the sinusoidal approximation and the measured signals after filtering.

These estimation results except $\hat{T}_A$ were summarized in Table 1. For the frequency estimation, the average of two peak frequencies in front and rear wheel orientation was selected. The sinusoidal graphs using these parameters are depicted by dotted lines in Fig. 8, Fig. 9 and Fig. 10 as well as Fig. 4 to Fig. 6.

3.4 Simulation for torque estimation

The amplitude of the yaw moment $\hat{T}_A$ cannot be measured in our experimental setup. Thus, we estimated it using dynamical simulations of a reduced-order model. For the simulation, a fourth-order Runge-Kutta method was applied with the step size 1/120 s. The parameters were set based on the actual board: M_b = 5kg is the board mass and $I_b = M_b(\ell^2 + w^2)/12$ is the moment of inertia. Here, ℓ = 0.8 m is the board length and w = 0.2m is the board width.

In the simulation, the yaw moment was changed in increments of 0.1 Nm, and the root mean square of the error between the measurement and simulation data was computed as an evaluation. Then, the yaw moment that gives the smallest evaluation was selected as $\hat{T}_A$. The obtained values in each trial are also shown in the rightmost row of Table 1.

In addition, the simulation results using input signals (1)-(4) with the parameters of the fifth trial in Table 1 are depicted in Figure 8. Although the simulated and measured data of the lateral deviation and the board orientation did not matched well, the traveling distance to the goal direction, which was selected for the evaluation for $\hat{T}_A$ estimation, showed similar trajectories.

These results demonstrate that the sinusoidal inputs for two-wheel orientations, normal force, and the yaw moment can propel a reduced-order model of a two-wheeled skateboard.

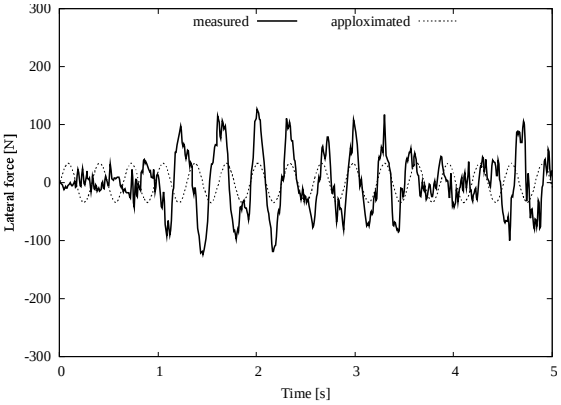

Fig.10 Reconstruction of lateral force.

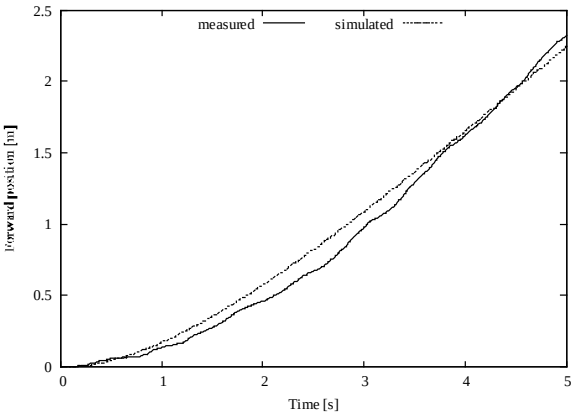

Fig. 11 Traveling distance.

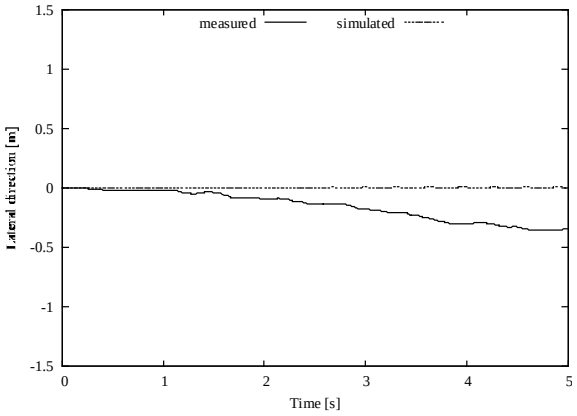

Fig.12 Lateral deviation.

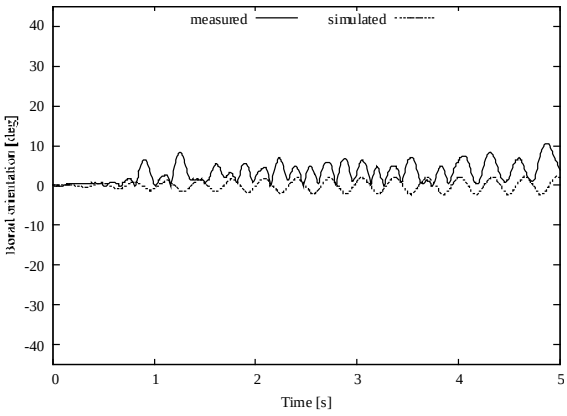

Fig.13 board Orientation.

5. CONCLUSION

In this paper, a two-wheeled skateboard motion was measured to obtain the input data to a reduced-order model. Using sinusoidal function, the data of the wheel orientation, the lateral force were reconstructed by regression, and a yaw moment was estimated based on the computer simulations. As a result, sinusoidal inputs can propel the two-wheeled skateboard.

The coincidence of the time-based trajectory to the goal direction implies the validity of a reduced-order model of the two-wheeled skateboard. However, the variation of the estimated parameters is not so small. In Table 1, although the motion frequency is commonly 3 Hz, both positive and negative values are found for the other parameters. In the first trial, where the data largely deviates from the other trials, a multipeak curve was observed in the power spectrum analysis (not shown in this paper). This fluctuation of the motion frequency enlarges the phase deviation in the sine regression from the measured data. Consequently, a slight decline in the frequency largely affects the phase and amplitude estimation. To obtain consistent data, it is desirable that the subject is proficient in producing the precise periodic motion of the skateboard.

In our future works, we have to experimentally confirm these findings, and develop the control method so as to include the lateral balance of the skateboard. Finally, we challenge to apply such a travelling method to actual manoeuvrability of the robot.

ACKNOWLEDGEMENTS

Part of this study was supported by "Gifu University Activation Grant" and "Grant-in-Aid for Scientific Research (C) (No. 22500173)".

REFERENCES

[1] M. Hubbard, "Human control of the skateboard", *J. Biomechanics*, Vol. 13, pp. 745-754, 1980.

[2] Y. Ispolov, B. Smolnikov, "Skateboard dynamics", *Computer Methods in Applied Mechanics and Engineering*, Vol. 131, pp. 327-333. 1996.

[3] K M. Lynch, "Optimal control of the thrusted skate", Automatica, Vol. 39, pp. 173-176, 2003.

[4] A.S. Kuleshov, "Mathematical model of a skateboard with one degree of freedom", *Doklady Physics*, Vol.52, pp283-286, 2007.

[5] A. Lewis, J. Ostrowski, J. Burdick, R. Murray, "Nonholonomic mechanics and locomotion: the snakeboard example", *Proceedings of the 1994 IEEE International Conference on Robotics and Automation*, pp. 2391-2400. 1994.

[6] J. Marsden, , J. Ostrowski, "Symmetries in motion: Geometric foundations of motion control". *Nonlinear Science Today*, pp. 1-21, 1998.

[7] J. Ostrowski, J. P. Desai, V. Kumar, "Optimal gait selection for nonholonomic locomotion systems", *The International Journal of Robotics Research*, Vol. 19, pp. 225-237, 2000.

[8] F. Bullo, A.Lewis, "Kinematic controllability and motion planning for the snakeboard", IEEE Transactions on Robotics and Automation, Vol.19, pp. 494-498, 2003

[9] S. Iannitti, K. M. Lynch, "Minimum control-switch motions for the snakeboard: A case study in kinematically controllable underactuated systems", *IEEE Transactions on Robotics*, Vol. 20, pp. 994-1006, 2004.

[10] Y. Golubev, "A method for controlling the motion of a robot snakeboarder", *Journal of Applied Mathematics and Mechanics*, Vol. 70, pp. 319-333, 2006

[11] E. Shammas, H. Choset, A. Rizzi , "Towards automated gait generation for dynamic systems with non-holonomic constraints", *Proceedings of the 2006 IEEE International Conference on Robotics and Automation*, pp. 1630-1636, 2006. [11] A. Asnafi, , M. Mahzoon, "Some flower-like gaits in the snakeboard's locomotion". *Nonlinear Dynamics*, Vol. 48,pp. 77-89, 2007.

[12] A. S. Kuleshov. "Further development of the mathematical model of a snakeboard", *Regular and Chaotic Dynamics*, Vol. 12, pp. 321-334, 2007

[13] J. Grabowski, M. de Leon, J. Marrero, D. de Diego, "Nonholonomic constraints: A new viewpoint", *Journal of Mathematical Physics*, Vol. 50, pp. 013520, 2009.

[14] T. Narikiyo, "Control of underactuated mechanical systems via passive velocity field control: Application to snakeboard and 3D rigid body", *Nonlinear Analysis*, Vol. 71, e2358-e2365, 2009.

[15] A. D. Lewis, "Simple mechanical control systems with constraints", IEEE Transactions on Automatic Control, Vol. 45, pp. 1420-1436, 2000.

[16] F. Bullo, M. Zefran, "On mechanical control systems with nonholonomic constraints and symmetries", *Systems and Control Letters*, Vol. 45, pp 133-144, 2002.

[17] S. Chitta, P. Cheng, E. Frazzoli, V. Kumar, "Robotrikke: A novel undulatory locomotion system", *IEEE International Conference on Robotics and Automation.* Vol. 2, p. 1597, 2005

[18] S. Ferraro, D. Iglesias, D. de Diego. "Momentum and energy preserving integrators for nonholonomic dynamics", *Nonlinearity*, Vol. 21, pp 1911-1928, 2008

[19] A. Astolfi, R. Ortega, A. Venkatraman, "A globally exponentially convergent immersion and invariance speed observer for mechanical systems with non-holonomic constraints". *Automatica* Vol. 46, pp. 182-189, 2010.

[20] S. Ito and H. Kawasaki, "Regularity in an environment produces an internal torque pattern for biped balance control", *Biological cybernetics*, Vol. 92, No. 4, pp. 241-251, 2005